Modelling the Inorganic Bromine Partitioning in the Tropical Tropopause over the Eastern and Western Pacific Ocean.

Maria A. Navarro[1], Alfonso Saiz-Lopez[2], Carlos A. Cuevas[2], Rafael P. Fernandez[3], Elliot Atlas[1], Xavier Rodriguez-Lloveras[2], Douglas Kinnison[4], Jean-Francois Lamarque[4], Simone Tilmes[4],Troy Thornberry[5,6], Andrew Rollins[5,6], James W. Elkins[5], Eric J. Hintsa[5,6], and Fred L. Moore[5,6]

[1] Department of Atmospheric Sciences, RSMAS, University of Miami, Miami, Florida, USA
[2] Department of Atmospheric Chemistry and Climate, Institute of Physical Chemistry Rocasolano, CSIC, Madrid, Spain
[3] National Research Council (CONICET), FCEN-UNCuyo, UTN-FRM, Mendoza, Argentina
[4]Atmospheric Chemistry Observation & Modeling Laboratory, National Center for Atmospheric Research, Boulder, Colorado, USA
[5] National Oceanic & Atmospheric Administration, Earth System Research Laboratory, Boulder, Colorado, USA
[6] Cooperative Institute for Research in Environmental Science, University of Colorado, Boulder, Colorado, USA

Correspondence to: Maria A. Navarro (mnavarro@rsmas.miami.edu)

Abstract. The stratospheric inorganic bromine burden (Br_y) arising from the degradation of brominated very short-lived organic substances (VSL_{org}), and its partitioning between reactive and reservoir species, is needed for a comprehensive assessment of the ozone depletion potential of brominated trace gases. Here we present modelled inorganic bromine abundances over the Pacific tropical tropopause based on aircraft observations of VSL_{org} of two campaigns of the Airborne Tropical TRopopause EXperiment (ATTREX 2013 carried out over eastern Pacific and ATTREX 2014 carried out over the western Pacific) and chemistry-climate simulations (along ATTREX flight tracks) using the specific meteorology prevailing. Using the Community Atmosphere Model with Chemistry (CAM-Chem), we model that BrO and Br are the daytime dominant species. Integrated across all ATTREX flights BrO represents ~ 43 % and 48 % of daytime Br_y abundance at 17 km over the western and eastern Pacific, respectively. The results also show zones where Br/BrO >1 depending on the solar zenith angle (SZA), ozone concentration and temperature. On the other hand, BrCl and $BrONO_2$ were found to be the dominant night-time species with ~ 61% and 56 % of abundance at 17 km over the western and eastern Pacific, respectively. The western-to-eastern differences in the partitioning of inorganic bromine are explained by different abundances of ozone (O_3), nitrogen dioxide (NO_2), and total inorganic chlorine (Cl_y).

1 Introduction

The role of bromine in stratospheric ozone depletion has been discussed in several studies (Daniel et al., 1999; Hossaini et al., 2015; Prather and Watson, 1990; Salawitch et al., 2005; Wofsy et al., 1975). Many of these discuss the contribution of brominated very short-lived organic substances (VSL_{org}) like bromoform ($CHBr_3$), dibromomethane (CH_2Br_2), bromochloromethane (CH_2BrCl), dibromochloromethane ($CHBr_2Cl$) and bromodichloromethane ($CHBrCl_2$), in addition to

long-lived halons and methyl bromide, as an important source of stratospheric bromine. The reaction mechanisms of VSL_{org} that lead to the formation of inorganic bromine (Br_y) involve complex sets of reactions that have been described in previous modelling studies (Krysztofiak et al., 2012; Ordóñez et al., 2012; Hossaini et al., 2010). The chemistry is initiated mainly via reaction with OH and photolysis and leads to the formation of several unstable organic halogenated radicals. The fate of these radicals, and their mechanisms of reaction, are controlled by NO_x conditions and OH levels. In polluted environments (high NO_x regime) the radicals react to produce NO_2 or halogenated nitrates that can decompose, experience oxidation or photolysis, washout or react on surfaces. In "clean" environments (low NO_x regime) the radicals undergo a series of cross reactions (including reaction with HO_2) leading to the formation of several different products that can continue reacting with OH (or Cl), washout or photo-dissociate to form Br_y species as end product (Krysztofiak et al., 2012).

The implementation of the complex chemistry of very short-lived species in current models like the Community Atmospheric Model with Chemistry (CAM-Chem) has been simplified by assuming that Br_y is immediately formed from photo-oxidised VSL_{org} (Ordóñez et al., 2012). However, the challenge to simulate VSL_{org} observations and quantify their degradation products (Br_y = Br + BrO + HOBr + $BrONO_2$ + HBr + BrCl + $2Br_2$ + $BrNO_2$ + IBr) relies on other atmospheric processes that could modify this chemistry. For example, the location and timing of emissions, the transport dynamics and dehydration processes in the tropical tropopause layer (TTL) (Liang et al., 2010), and the occurrence of heterogeneous recycling reactions on sea-salt aerosol and ice-crystals (Fernandez et al., 2014). A recent study by Navarro et al. (2015), carried out in the TTL over the Pacific Ocean, showed the impact of strong convective events on the chemistry of brominated species. The estimates of the contribution of very short-lived substances to total stratospheric bromine over the tropical eastern and western Pacific, showed a similar amount of VSL_{org} over both regions. Nevertheless, a smaller amount of Br_y was observed over the western Pacific due to the influence of the South Pacific Convection Zone (SPCZ) and the path of typhoon Faxai in 2014.

As the tropical circulation, assisted by convection, could enhance the vertical transport of VSL_{org}, the VSL_{org} degradation products could reflect changes in their abundances and chemical speciation. A previous study by Fernandez et al. (2014) calculated that VSL_{org} provided an annual average tropical stratospheric injection of total bromine of approximately 5 ppt (parts per trillion), where ~ 3 ppt entered the stratosphere as a product gas, while ~2 ppt did so as a source gas. In this study, the distribution of Br_y species showed Br and BrO to be the dominant inorganic species during daytime, particularly over the tropical western Pacific, which was suggested to be a hot spot with increased stratospheric bromine injection (~3.8 ppt Br_y and ~3.8 ppt VSL_{org}). This study also introduced the concept of the "tropical ring of atomic bromine", a photochemical phenomenon that extends in the tropics from approximately 15 to 19 km where the abundance of Br atoms is favoured due to low temperatures (<200K) and low O_3 abundances (<100 ppb). Similarly, the estimates of stratospheric Br_y inferred from atmospheric measurements of BrO during the NASA- Airborne Tropical TRopopause EXperiment (ATTREX) deployment over eastern Pacific, showed approximately 3 to 5 ppt for potential temperatures between 350 and 400 K in the TTL (Werner et al., 2017).

Our study manly focuses on the difference in modelled Br_y concentrations in the TTL over the Pacific throughout the ATTREX campaign flight tracks, and examines its temporal and spatial distributions. Based on the reliable representation of the observed

VSL_{org} by the CAM-Chem model on the study of (Navarro et al., 2015), and as a follow up of this investigation regarding the chemistry of bromine tracers in the TTL, we estimated the partitioning of Br_y over the tropical eastern and western Pacific during 2013 and 2014, respectively. From this case study analysis, we also complemented the study of the diurnal Br_y speciation in the TTL, and the Br/BrO ratio distribution in the Upper Troposphere-Lower Stratosphere (UTLS) modelled by (Fernandez et al., 2014) and (Saiz-Lopez and Fernandez, 2016). This paper is organized as follows: Section 2 briefly describes the campaign, the methods used for the observations of trace gases, and the characteristics of the model simulations. Section 3 discusses the major findings regarding the amount of Br_y and its partitioning within the TTL, as well as its relevance for the formation of the proposed tropical ring of atomic bromine (Fernandez et al., 2014; Saiz-Lopez and Fernandez, 2016). In addition, Section 3 discusses the results of a sensitivity test in the model where water-ice aerosol reactions are deactivated. Section 4 summarizes and concludes this study.

2 Methods:

2 .1 Observations

2 .1. 1 ATTREX Campaign

ATTREX, an airborne campaign focused on the chemical and physical processes in the TTL (~13-18 km), took place over the Pacific Ocean during boreal winter (Jensen et al., 2015). In 2013, six flights were conducted over the eastern and central Pacific, targeting the area between 187 and 268 °E and 11 °S to 34 °N (hereafter referred to as the eastern Pacific (EP)). In 2014, eight flights were carried out over the western Pacific, covering the area between 120 and 165 °E and 11 °S to 35 °N (hereafter referred to as the western Pacific (WP)). On board the NASA Global Hawk, the University of Miami deployed the Global Hawk Whole Air Sampler (GWAS) to collect more than 900 samples at different locations along the flight tracks. From these measurements, 436 observations along the flight track (388 during the day and 48 at night) over the WP and 309 flight points (152 during the day and 157 at night) over the EP were used to simulate Br_y partitioning during NASA ATTREX campaigns (Fig 1). Due to the logistics of the missions, the distribution of sample points according to solar zenith angle (SZA) was different between WP and EP. During ATTREX 2014 (WP), flights occurred mostly during daylight hours, as the plane took off at early local morning (~17:00 UTC, 3:00 am local time). Also, flights lasted approximately 20 hours reducing the amount of night-time samples, particularly at high SZA. The legs went in different directions, mostly west-east, north-south, and even a local circle flight, following a different path from and to Andersen Air Force Base (13.5 °N, 144.9 °E). For these reasons, samples showed a high density of observations at 50° SZA, and no samples beyond 130° SZA for WP. In contrast, during ATTREX 2013 (EP), flights also took off during early morning (~15:00 UTC, 7:00 am local time), but lasted between 22 to 24 hours. In addition, the legs went in southern and south-western direction and came back to Edwards Air Force Base

(34.9 °N, 243.8 °E) over the same path. Hence, for the EP, the number of samples was evenly distributed along the entire range of SZAs.

2 .1. 2 VSL_{org} Observations

Measurements of VSL_{org}, were carried out with the GWAS during the deployments and were used here to evaluate the model. Detailed methodology and implementation of this instrument is described in (Navarro et al., 2015). Briefly, the GWAS counts with 90 custome-made stainless steel canister of 1.3 L. Two metal bellows pumps (Senior Aerospace) flow ambient air through a custome inlet at 2 to 8 liters per minute depending on the altitude. The instrument is fully automated and controlled from the ground through an Ethernet interface. During ATTREX mission, samples were collected along the Global Hawk flight track at different altitudes by closing the exhaust valves (Parker-Hannifin) and opening the solenoid valve (Parker-Hannifin) of the selected sample canister. When desired pressure was reached the canister valve closed and manifold continued flushing by sequentially opening the exhaust valve. After sample collection, canisters were analysed using a high-performance gas chromatograph (Agilent Technology 7890A) and mass spectrometer with mass selective, flame ionization and electron capture detector (Agilent Technology 5975C). The VSL_{org} bromine budget and the vertical distribution of these species were presented in a previous publication (Navarro et al., 2015) which also included estimates of the organic *vs.* inorganic bromine fraction over the EP and WP.

At the tropopause level (~17 km), the modelling estimates of the organic bromine fractions were similar for the entire Pacific (3.84 ± 0.64 and 3.18 ± 1.49 ppt from WP and EP, respectively). However, the inorganic fraction inferred from VSL_{org} measurements showed 3.02 ± 1.90 ppt of Br_y over the EP and 1.97 ± 0.21 ppt over WP (Navarro et al., 2015). Based on these results, we performed model simulations to look into the variability and distribution of the Br_y partitioning, and used ozone concentrations measured with the National Oceanic & Atmospheric Administration's Ozone system (NOAA-O_3) during ATTREX 2013, and the Unmanned aircraft system Chromatograph for Atmospheric Trace Species (UCATS-O_3) during ATTREX 2014 to also evaluate the model.

2 .1. 2 O_3 Observations

Measurements of ozone were carried out with dual-beam UV photometers. These instruments utilize two identical absorption cells, a mercury lamp, an ozone scrubbing catalyst, and two detectors that measure 253.7-nm UV radiation transmitted through the absorption cell. At this wavelength, the ozone absorption cross-section is well known, and thus the ozone number density can be readily calculated by Beer's Law. Since the two absorption cells are identical, virtually continuous measurements of ozone are made by alternating the ambient air sample and ozone scrubbed sample between the two of them. At a fast collection rate (from 2 Hz at < 200hPa to 0.5 Hz at 500hPa for NOAA- O_3 and 0.2 Hz for UCATS-O_3), the minimum detectable concentration of ozone corresponds to 1 ppb or less at STP. Based on an intercomparison between the two instruments during

ATTREX 2013, the UCATS-O_3 instrument was 4.8±0.8 ppb higher than NOAA-O_3 in the regions of interest between 50 and 250 ppb, and approached zero near 500 ppb. The NOAA-O_3 instrument was unavailable on ATTREX-2014. These continuous measurements of ozone were averaged to match the location where GWAS samples were collected, and then compared to CAM-Chem outputs.

2 .2 Modelling: CAM-Chem configuration

The estimations of VSL_{org}, O_3 and the Br_y partitioning were carried out with the CAM-Chem model, a 3-D chemistry climate model included into the CESM framework (Community Earth System Model, version 1.1.1) (Lamarque et al., 2012). This model includes a complete photochemistry, wet and dry deposition and heterogeneous chemistry on sea-salt aerosols and ice particles (Fernandez et al., 2014; Ordóñez et al., 2012). The current setup is based on the bromo- carbon emission inventory of Ordoñez et al., (2012), which includes time-dependent geographically distributed sources of $CHBr_3$, $CH2Br_2$, CH_2BrCl, $CHBr_2Cl$, $CHBrCl_2$ and CH_2IBr. Even when we do not consider here other chloro-carbon sources like CH_2Cl_2 and C_2Cl_4, those species live long enough to be injected almost entirely as source gases to the stratosphere and do not contribute to the tropospheric inorganic chlorine (Cl_y) loading (Hossaini et al., 2015). Additional Br_y and Cl_y sources from sea-salt heterogeneous dehalogenation in the lower troposphere are parameterized (Ordóñez et al., 2012; Fernandez et al., 2014). Prescribed surface volume mixing ratios of long-lived chlorofluorocarbons (CFCs) and halons, as well as surface concentration of anthropogenic CO_2, CH_4, N_2O and other ozone precursors are based on the long-lived inventory of (Meinshausen et al., 2011).

Model simulations were run in specified dynamics mode (SD) using meteorological fields prevailing at the time of the campaigns. A spatial resolution of 1° (longitude) x 1° (latitude) with 56 vertical levels (from the surface to ~ 3.5 hPa) and a temporal resolution of 30 min were used. Model hourly output was sampled at exactly the same times and locations as the ATTREX measurements, without performing neither spatial nor temporal averaging on model grids. Once each independent flight track was extracted from the model output, all atmospheric quantities were averaged into 1 km altitude bins, to compare with measured data. The chemistry of Br_y species between the daytime and night-time was distinguished by disregarding the samples collected during twilight (total solar zenith angle between 80° and 100°). In addition, local estimations of ozone, nitrogen dioxide and inorganic chlorine concentrations were carried out over the EP and WP along the flight tracks to understand the chemistry that leads to the specific bromine partitioning.

3 Results and discussion

This modelling study was carried out simultaneously with the work published by (Navarro et al., 2015). Only ozone and VSL_{org} abundances were available to validate model performance as BrO and NO_2 measurements from the ATTREX mission, now published by (Werner et al., 2017), were still under examination by the time of this analysis. Thus, once the model performance

during ATTREX campaign is evaluated in Sect. 3.1, we step into a CAM-Chem modelling case study oriented to determine the Br_y partitioning (Sect. 3.2) and efficiency of heterogeneous recycling reactions (Sect- 3.3) on the mostly unexplored eastern and western Pacific TTL.

3. 1 CAM-Chem model evaluation

The first step of this study was to evaluate the CAM-Chem model to substantiate that its chemistry and other components show a satisfactory performance, and that its results are consistent with the intended application. We used the NOAA-O_3, UCATS-O_3, and organic bromine species from GWAS measurements taken during the ATTREX campaign, since BrO and NO_2 measurements from the ATTREX mission were still under examination by the time of this analysis. Figure 2 shows the measurements and model mixing ratios of O_3 in the Upper Troposphere-Lower Stratosphere (UTLS) for both, the WP and EP respectively. The NOAA and UCATS O_3 mixing ratios averaged into 1 km altitude bins ranged from 46 ppb at 14 km to 166 ppb at 18km over the WP, and 46 ppb to 179 ppb from 14 to 18 km over EP; while CAM-Chem simulations estimated 67 ppb to 196 ppb from 14 to 18 km over WP, and 100 ppb at 14 km and 243 ppb at 18 km over EP. The model reproduces well the variability of measured ozone with altitude in both the WP and EP. However, the different convective processes are not accurately represented for in both regions, leading to an offset in the EP between measurements and simulated ozone values. The vertical profile of organic bromine species from GWAS measurements can be found in a previous publication (Navarro et al., 2015).

Figure 3 shows the correlation between average measurements and model outputs of the 1 km of altitude bins for O_3, $CHBr_3$ and CH_2Br_2 over the WP and EP. Excellent correlation ($R^2 > 0.97$) between O_3 measurements and CAM-Chem estimates for both EP and WP were observed, with slopes not differing significantly from unity. However, small vertical offsets in the "y" axis (27.1 ppb in WP and 54.5 ppb in EP) reflect the simulated bias in the model. In addition, good agreement was observed between GWAS measurements and model simulations of $CHBr_3$ ($R^2 = 0.84$ for WP, $R^2 = 0.81$ for EP), and CH_2Br_2 ($R^2 = 0.95$ for WP, $R^2 = 0.90$ for EP), as shown in figure 3 and the previous work of (Navarro et al., 2015).

3. 2 Br_y partitioning

The vertical distribution of inorganic species showed a slight variability with altitude (Fig 4). Over both the WP and the EP, BrO and Br prevail at daytime hours from 14 to 18 km. However, below 16 km, the amount of HBr present over the EP tends to be slightly larger than that of atomic Br. For the WP and the EP during night-time hours, BrCl and $BrONO_2$ are the dominant species in agreement with (Fernandez et al., 2014). Mixing ratios of BrCl closely compete with $BrONO_2$, particularly at 15 and 18 km over the WP. Over the EP, $BrONO_2$ dominates the entire range of altitude from 14 to 18 km. The total Br_y burden during daylight hours increases from 1.49 to 2.43 ppt between 14 km and 18 km over the WP and from 1.82 to 2.97 ppt over the EP

within the same altitude range. On the other hand, night-time Br_y ranges from 1.40 to 2.27 ppt and 1.82 to 2.99 ppt for the WP and EP, respectively. This indicates that the total Br_y atmospheric burden is equivalent within the diurnal cycle. Note that within the same altitude range, the model output for total VSL_{org} decreases from 5.72 ppt at 14 km to 2.53 ppt at 18 km over the WP, and from 3.90 ppt at 14 km to 1.97 ppt at 18 km over the EP, indicating the dominant role played by VSL photodecomposition in controlling the Br_y loading in the tropical UTLS (Navarro et al., 2015). Our mean vertical distributions for the EP are in the lower edge of the reported ranges of (Werner et al., 2017), who reported a measured range for BrO between 0.5 ± 0.5 ppt at the bottom of the TTL and about 5 ppt at θ = 400 K, consistent with an inferred increase of Br_y from a mean of 2.63 ± 1.04 ppt to 5.11 ± 1.57 ppt as we move upward in the TTL.

At the tropopause level (~17 km) and integrated over all flights and SZAs, the inorganic partitioning showed ~ 43 % (0.79 ppt) of abundance of BrO during daylight and ~61 % of BrCl (0.94 ppt) during night-time over WP. On the other hand, 48 % (1.43 ppt) of Br_y is presented as BrO during daylight and 56 % (1.41 ppt) as $BrONO_2$ at night-time over EP (Fig 4). Atomic bromine is the second most abundant species during the day, with mean daytime values of 0.64 ppt and 0.57 ppt for the WP and EP, respectively. During the night, $BrONO_2$ (0.29 ppt) and BrCl (0.34 ppt) are the 2nd most abundant species over the WP and EP, respectively. It is worth noting that even when the maximum inorganic chlorine levels are larger in the EP, BrCl is not the dominant night-time reservoir, while in the WP, where BrCl dominates, maximum Cl_y mixing ratio is almost half the value found in the EP (see Table 1). Considering all flights, the maximum Cl_y abundances are < 85 pptv in the WP and < 182 for the EP, with a global mean tropical annual Cl_y mixing ratio of 50 pptv in agreement with previous reports (Marcy et al., 2004; Mébarki et al., 2010). This can be explained considering the faster vertical transport occurring in the western pacific region, which decreases the contribution from photochemical decomposition of VSL chlorocarbons (Saiz-Lopez and Fernandez, 2016).

In order to understand the chemistry that led to these abundances, the concentrations of Br_y products (Br, BrO, HOBr, $BrONO_2$, HBr, and BrCl), as well as modelled mixing ratios of the dominant reactants: O_3, NO_2, and Cl_y, were studied as a function of the SZA for the entire range of altitude (14 to 18 km). Figure 5 compares the mean abundances observed in the EP and WP considering all flights. Even when these results are not descriptive of each independent flight, they are representative and illustrative of the mean state of the tropical upper atmosphere within the eastern and western Pacific in the presence and absence of sunlight. Equivalent results but for each independent flight are shown in the Supplementary Online Material. According to the results, during the daylight hours, the high abundance of average O_3 (up to ~ 190 ppb), compared to average NO_2 and Cl_y (Cl_y up to ~ 84 ppt, NO_2 up to ~ 33 ppt) (Fig 5b), led to the rapid formation of BrO over the WP (Fig 5a). As the SZA keeps on increasing, a decrease on photolysis as well as ozone concentrations (particularly at SZA ~ 100-120°, Fig 5b) allow the heterogeneous reaction of the inorganic chlorine (mostly HCl) and bromine reservoirs (HOBr and $BrONO_2$) to increase the production of BrCl during the night-time hours. Note that the accumulation of night-time BrCl is more evident during ATTREX 2014 due to the larger ice-crystals surface areas and lower NO_x levels prevailing over the WP (Fig 5a).

The scenario over the EP is slightly different as levels of NO_2 and O_3 define a high NO_x regime. A statistical analysis of CAM-Chem NO_2 model estimations during daylight over the EP is presented in Fig 6. Our average range of NO_2 mixing ratios is

approximately 15 ± 6 ppt at 14 km, with slightly higher values over the tropopause, 22 ± 24 ppt at 17 km. These estimates within 1 standard deviation agree with the NO_2 values presented by Stutz et al. (2016) and (Werner et al., 2017) from observations made during ATTREX 2013 over the EP. As they report in their manuscript, their O_3 scaling technique allowed retrieval of NO_2 concentrations of 15 ± 15 ppt in the TTL, and a range of 70 up to 170 ppt in the mid-latitude lower stratosphere. However, previous studies have shown large associated uncertainties in TTL NO_2 measurements based on remote sensing instruments ((Weidner et al., 2005; Butz et al., 2006; Bauer et al., 2012)).

Hence, the EP daytime average concentrations of ozone (up to ~ 300 ppb), Cl_y (max Cl_y ~ 181 ppt) and NO_2 (max NO_2 ~ 48 ppt) are almost twice as high as those over the WP (Fig 5d). Higher concentrations of ozone were associated with enhanced production of BrO (Fig 5c). Meanwhile, during dark hours, the high concentrations of NO_2 (up to ~ 210 ppt) (Fig 5d), lead to the predominant formation of $BrONO_2$ over the EP (Fig 5c). These results are in good agreement with the partitioning of Br_y found by (Werner et al., 2017) where BrO is the daylight dominant species over EP, and the estimates of Fernandez et al. (2014), which suggested BrO and $BrONO_2$ as the dominant species in the TTL over the entire tropics during daytime and midnight, respectively.

Note that the differences in Cl_y abundance can reach factors as much as 5 times larger for the EP if the independent flights are considered (e.g., max. Cly ~500 ppt for RF01, RF03 and RF04 performed in the EP during ATTREX-2013, while max. Cl_y for all flights except RF07 (< 400 pptv) remain below 100 ppt). However, the night-time BrCl abundance is still larger in the WP, representing more than 90% of the night-time Br_y partitioning for flights RF02 and RF04 (see Figure S1 & S2 in the Supplement). For these cases, BrCl mixing ratios between 1 and 2 pptv are modelled within air-parcels with a very low Cl_y abundance (of the order of 10 ppt). In order to understand this unexpected behaviour, we performed a sensitivity simulation neglecting the inter-halogen heterogeneous recycling occurring on upper tropospheric ice-crystals, see Sect. 3.3 below.

3. 2. 1 Tropical ring of atomic Br: indications from this case study

Our results also indicate that, integrated over all SZAs, the second most abundant species over both EP and WP during daytime is atomic Br. This species plays a fundamental role in the formation of the proposed inhomogeneous tropical ring of atomic Br, a natural atmospheric phenomenon that comes from the rapid photochemical equilibrium between BrO and Br under low O_3 and temperatures (Fernandez et al., 2014; Saiz-Lopez and Fernandez, 2016). According to our estimations, during daytime hours, the average mixing ratios of Br remain below 0.75 ppt over the EP and WP along the entire range of altitudes (i.e., between 14 to 18 km) (Fig 4). Note, however, that atomic Br abundances surpass BrO mixing ratios at low SZA (close to noontime) and low ozone abundances (below 100 ppb, Fig. 5b and 5d). These observations contrast with the variability observed in BrO, whose mixing ratios vary from 0.61 ppt up to 1.19 ppt over WP and from 0.72 ppt to 1.43 ppt over EP (Fig 4), depending on O_3 and NO_2 background levels. Also note that Br shows a smooth variation during the day, slightly decreasing its abundance as the SZA increases, while the temporal evolution of BrO is more variable, mostly under the high NO_x regime

prevailing in the EP (Fig. 5). A closer inspection on each independent flight (Figs. S1 and S2) reveals the large inhomogeneity of the tropical rings of atomic bromine. In the EP, Br surpasses BrO mixing ratios at 60º SZA for flights RF04 and RF06, but as the remaining flights sampled larger BrO mixing ratios, the mean EP abundances shown in Fig. 5c shows Br/BrO > 1 only at 20º SZA. Similarly, the mean results shown in Fig. 5a for the WP show BrO > Br at all times, but RF02 and RF03 show the ratio Br/BrO to be larger than one at 50º SZA. This highlights the importance of considering non-averaged (both spatially and temporally) model output to determine the concentration of photochemical reactive species or other atmospheric quantities such as the Br/BrO ratio.

In contrast to the study of (Werner et al., 2017), which focused on ATTREX measurements taken exclusively over the EP and used an O_3-scaling technique to retrieve their results, our model calculations support the fact that the Br/BrO ratio could become larger than the unity, particularly in the tropical UT and TTL of both, eastern and western Pacific Ocean during daylight hours, particularly at low SZA. Nevertheless, the combination of ozone concentrations and temperatures plays a fundamental role in the distribution of both species, thus it is expected to find a spatially irregular pattern in the conditions that favour Br/BrO > 1.

Figure 7 shows the distribution of the Br/BrO ratio over the WP and EP, and its correlation with ozone concentrations and temperatures. The results are based on the mean 1 km binned data for all track flights, although equivalent conclusions can be drawn for each independent transect. Over the EP, Br/BrO > 1 are observed as discrete masses, particularly at SZA between 40° and local noon. Note that cold temperatures and low O_3 concentrations enhance the prevalence of atomic Br for those times and locations. Indeed, (Saiz-Lopez and Fernandez, 2016), determined that Br becomes the dominant species for O_3 < 100 ppb and T < 200 K. Br/BrO ratios lower than 1 are observed near the tropopause for SZA between 40° and 55° under higher concentrations of ozone and warmer temperatures. The Br/BrO distribution over the WP seems to be more inhomogeneous with an overall higher Br/BrO ratio than over the EP. This overall lower ratio Br/BrO in the EP compared to WP could be due to the higher levels of O_3 modelled in this region (Fig. 2). In any case, the presence of the tropical rings of Br occurs as a spotted/patchy stamp of bromine atoms superposed on top of a background BrO curtain. In general, the Br/BrO ratio peaks at 17 km, very close to the upper limit of the TTL, highlighting the importance of determining Br abundances in order to address the total amount of Br_y injected to the stratosphere.

As the magnitude of the Br_y reactive species (Br and BrO) depends on changes in the oceanic sources and vertical transport, the Br/BrO ratio will vary according to the seasons and geographical regions. Hence, during strong convective events over the WP (e.g., air masses tracked from the SPCZ) the amount of Br and BrO remained similar to each other. These results are in good agreement with the statements of Fernandez et al. (2014), which suggested Br/BrO > 1 during strong convective periods over the WP warm pool region.

Reservoir species like HBr and HOBr were the third most dominant substances. These two species contribute to the formation of BrCl through heterogeneous recycling reactions (see (Ordóñez et al., 2012)), particularly at night due to the absence of photolysis reactions and the presence of trace chlorine. As suggested by Fernandez et al. (2014), higher abundances of Cl_y,

could result from the decomposition of very short-lived chlorocarbons or the subsidence of HCl from the stratosphere to the TTL, driving the night-time chemistry in areas where $Cl_y > Br_y$.

3. 3 Heterogeneous reactions: impact of water-ice recycling on Br_y speciation/distribution

Heterogeneous recycling reactions of reservoir species on ice-crystals are relevant at UTLS levels, thus, a sensitivity test was carried out to determine the influence of water-ice aerosols on the distribution of the inorganic species. Equations (1) to (6) shows the chlorine, bromine and inter-halogen tropospheric heterogeneous reactions occurring on ice-crystals (for a complete description of the implementation of heterogeneous reactions in CAM-Chem, see Table S1 in supplementary online material of (Fernandez et al., 2014).

$$BrONO_2 \rightarrow HOBr + HNO_3 \quad (1)$$
$$ClONO_2 \rightarrow HOCl + HNO_3 \quad (2)$$
$$HOCl + HCl \rightarrow Cl_2 + H_2O \quad (3)$$
$$HOCl + HBr \rightarrow BrCl + H_2O \quad (4)$$
$$HOBr + HCl \rightarrow BrCl + H_2O \quad (5)$$
$$HOBr + HBr \rightarrow Br_2 + H_2O \quad (6)$$

Figure 8 shows mixing ratios at different altitudes when water-ice aerosol reactions were deactivated simultaneously. Relative to the results from the complete mechanism (Fig. 4), at 17 km, the absence of ice-crystal reactions increases the total inorganic fraction by 7% and 12% over the EP during the day and night, respectively. On the other hand, Br_y increases by 29% and 40% over the WP during day and night, respectively. This relative increase of total Br_y is mainly due to changes in the amount of HBr and BrCl. Note that the mixing ratio of all species, except for HBr (and $BrONO_2$ during night-time) remain similar when comparing Figure 4 and Figure 8. As explained by Aschmann et al. (2011) the increment in the amount of HBr at high altitude levels could be due to a slowly sedimentation following by evaporation as the adsorbed HBr is not washed out right away. Another characteristic of the sensitivity test is the clear absence of BrCl during night-time as water-ice aerosol reactions of HOBr and HCl are suppressed. Comparing to the base case, the absence of BrCl makes $BrONO_2$ the dominant species at night over the WP, with 53% at 17 km, compared to 61% BrCl in the base case. Thus, neglecting ice-recycling reactions (1) to (6) prevents the heterogeneous conversion of $BrONO_2$ to BrCl, and gas-phase bromine nitrate (which is formed mainly by the termolecular reaction of $BrO + NO_2 + M$ during twilight) remain as the dominant Br_y species during the night both under a high-NO_x regime (i.e., within the EP region) as well as under the relatively low-NO_x regime (western pacific). But when the heterogeneous recycling reactions are activated, the model predicts that the recycling efficiency depends mostly on the total surface area density of ice-crystals in the upper troposphere (SAD-ICE): even under very low Cl_y concentrations (between 10

and 20 ppt), if SAD-ICE is present in the TTL, the night-time reservoir partitioning is shifted to BrCl. Fernandez et al., (2014) found tropospheric SAD-ICE levels within the western pacific upper TTL to be some of the largest within the tropics, suggesting that BrCl abundance should peak in this region of the pacific. However, the heterogeneous chemistry of bromine species with water-ice aerosols still requires further research as their atmospheric surfaces are highly dynamic. The presence of cirrus ice clouds, at the cold temperatures of the equatorial and mid-latitude UTLS, facilitates the conversion of bromine reservoir species to more photochemically active forms, which play an important role in the oxidative capacity of this region of the atmosphere.

4 Summary and Conclusions

Our estimates of the Br_y partitioning at the tropical tropopause over the Pacific Ocean showed BrO and atomic Br to be the dominant species during daytime hours, while BrCl and $BrONO_2$ were found as the night-time dominant species over the WP and EP, respectively. The difference in the partitioning of Br_y during the diurnal cycle could be explained by the changes in the abundance of O_3, NO_2 and Cl_y in these two regions of the Pacific, as well as the efficiency of heterogeneous reactions that could modify this chemistry, mostly during the night. Table 1 show a summary of the results found at 17 km.

Reactive species like atomic Br become the dominant Br_y species in large regions of the TTL during daylight, following the large variation of ozone abundance within these regions strongly influenced by deep convection. The low ozone and cold conditions, in combination with the rapid photochemical equilibrium between BrO and Br, favour Br/BrO > 1 and support previous results about the proposed tropical ring of atomic bromine. Within the ATTREX flights, both Br and BrO alternate as the dominant daytime species, indicating a large inhomogeneity for the tropical ring of Br, mainly due to the large ozone/T variability of the air parcels within the convective tropical WP and EP. Nevertheless, improved field data for the speciation of bromine are evidently needed to continue evaluating this hypothesis.

The degradation of VSL_{org}, their transport into the TTL, as well as the efficiency of heterogeneous reactions involving ice aerosols, play an important role in the overall atmospheric loading of Br_y, both reactive and reservoir species. This model study contributes to the growing database of reactive halogen estimates based on halocarbon observations. However, further research on the organic/inorganic bromine fraction, as well as its distribution between reactive and reservoir species, is needed in different areas of the globe and at different heights to diminish the uncertainty of the amount of Br_y that reaches the stratosphere, and properly constraint the global bromine budget.

Acknowledgments

This work was supported by NASA Grant NNX10AO83A S08 and NASA Atmospheric Composition Modelling and Analysis Program Activities (ACMAP), grant/cooperative agreement number NNX11AH90G.

We gratefully acknowledge the support of Eric Jensen and Lenny Pfister, principal investigators of the ATTREX campaign. We thanks the engineers, technicians and pilots of NASA Armstrong Flight Research Center, and NASA-ESPO Project

Management, as well as S. Schauffler, R. Lueb, R. Hendershot and S. Gabbard for technical support in the field, and V. Donets, X. Zhu and L. Pope for GWAS data analysis. The National Center for Atmospheric Research (NCAR) is funded by the National Science Foundation NSF. Computing resources (ark:/85065/d7wd3xhc) were provided by the Climate Simulation Laboratory at NCAR's Computational and Information Systems Laboratory (CISL), sponsored by the NSF and other agencies. The CESM project (which includes CAM-Chem) is supported by the NSF and the Office of Science (BER) of the US Department of Energy. RPF would like to thanks CONICET and FCEN-UNCuyo/UTN-FR Mendoza for financial support.

References

Aschmann, J., Sinnhuber, B.-M., Chipperfield, M., and Hossaini, R.: Impact of deep convection and dehydration on bromine loading in the upper troposphere and lower stratosphere, Atmospheric Chemistry and Physics, 11, 2671-2687, 2011.

Bauer, R., Rozanov, A., McLinden, C., Gordley, L., Lotz, W., Russell III, J., Walker, K., Zawodny, J., Ladstätter-Weißenmayer, A., and Bovensmann, H.: Validation of SCIAMACHY limb NO 2 profiles using solar occultation measurements, Atmospheric Measurement Techniques, 5, 1059-1084, 2012.

Butz, A., Bösch, H., Camy-Peyret, C., Chipperfield, M., Dorf, M., Dufour, G., Grunow, K., Jeseck, P., Kühl, S., and Payan, S.: Inter-comparison of stratospheric O 3 and NO 2 abundances retrieved from balloon borne direct sun observations and Envisat/SCIAMACHY limb measurements, Atmospheric Chemistry and Physics, 6, 1293-1314, 2006.

Daniel, J., Solomon, S., Portmann, R., and Garcia, R.: Stratospheric ozone destruction: The importance of bromine relative to chlorine, Journal of Geophysical Research: Atmospheres (1984–2012), 104, 23871-23880, 1999.

Fernandez, R., Salawitch, R., Kinnison, D., Lamarque, J.-F., and Saiz-Lopez, A.: Bromine partitioning in the tropical tropopause layer: implications for stratospheric injection, Atmospheric Chemistry and Physics, 14, 13391-13410, 2014.

Hossaini, R., Chipperfield, M., Monge-Sanz, B., Richards, N., Atlas, E., and Blake, D.: Bromoform and dibromomethane in the tropics: a 3-D model study of chemistry and transport, Atmospheric Chemistry and Physics, 10, 719-735, 2010.

Hossaini, R., Chipperfield, M., Montzka, S., Rap, A., Dhomse, S., and Feng, W.: Efficiency of short-lived halogens at influencing climate through depletion of stratospheric ozone, Nature Geoscience, 2015.

Jensen, E. J., Pfister, L., Jordan, D. E., Bui, T. V., Ueyama, R., Singh, H. B., Thornberry, T., Rollins, A. W., Gao, R.-S., and Fahey, D. W.: The NASA Airborne Tropical TRopopause EXperiment (ATTREX): High-altitude aircraft measurements in the tropical western Pacific, Bulletin of the American Meteorological Society, 2015.

Krysztofiak, G., Catoire, V., Poulet, G., Marécal, V., Pirre, M., Louis, F., Canneaux, S., and Josse, B.: Detailed modeling of the atmospheric degradation mechanism of very-short lived brominated species, Atmospheric Environment, 59, 514-532, 2012.

Lamarque, J. F., Emmons, L. K., Hess, P. G., Kinnison, D. E., Tilmes, S., Vitt, F., Heald, C. L., Holland, E. A., Lauritzen, P. H., Neu, J., Orlando, J. J., Rasch, P. J., and Tyndall, G. K.: CAM-chem: description and evaluation of interactive atmospheric chemistry in the Community Earth System Model, Geosci. Model Dev., 5, 369-411, 10.5194/gmd-5-369-2012, 2012.

Liang, Q., Stolarski, R., Kawa, S., Nielsen, J., Douglass, A., Rodriguez, J., Blake, D., Atlas, E., and Ott, L.: Finding the missing stratospheric Br y: a global modeling study of CHBr 3 and CH 2 Br 2, Atmospheric Chemistry and Physics, 10, 2269-2286, 2010.

Marcy, T. P., Fahey, D. W., Gao, R. S., Popp, P. J., Richard, E. C., Thompson, T. L., Rosenlof, K. H., Ray, E. A., Salawitch, R. J., Atherton, C. S., Bergmann, D. J., Ridley, B. A., Weinheimer, A. J., Loewenstein, M., Weinstock, E. M., and Mahoney, M. J.: Quantifying Stratospheric Ozone in the Upper Troposphere with in Situ Measurements of HCl, Science, 304, 261-265, 10.1126/science.1093418, 2004.

Mébarki, Y., Catoire, V., Huret, N., Berthet, G., Robert, C., and Poulet, G.: More evidence for very short-lived substance contribution to stratospheric chlorine inferred from HCl balloon-borne in situ measurements in the tropics, Atmos. Chem. Phys., 10, 397-409, 10.5194/acp-10-397-2010, 2010.

Meinshausen, M., Smith, S. J., Calvin, K., Daniel, J. S., Kainuma, M. L. T., Lamarque, J. F., Matsumoto, K., Montzka, S. A., Raper, S. C. B., Riahi, K., Thomson, A., Velders, G. J. M., and van Vuuren, D. P. P.: The RCP greenhouse gas concentrations and their extensions from 1765 to 2300, Clim. Change, 109, 213-241, 10.1007/s10584-011-0156-z, 2011.

Navarro, M. A., Atlas, E. L., Saiz-Lopez, A., Rodriguez-Lloveras, X., Kinnison, D. E., Lamarque, J.-F., Tilmes, S., Filus, M., Harris, N. R., and Meneguz, E.: Airborne measurements of organic bromine compounds in the Pacific tropical tropopause layer, Proceedings of the National Academy of Sciences, 112, 13789-13793, 2015.

Ordóñez, C., Lamarque, J.-F., Tilmes, S., Kinnison, D. E., Atlas, E. L., Blake, D. R., Sousa Santos, G., Brasseur, G., and Saiz-Lopez, A.: Bromine and iodine chemistry in a global chemistry-climate model: description and evaluation of very short-lived oceanic sources, Atmospheric Chemistry and Physics, 12, 1423-1447, 2012.

Prather, M. J., and Watson, R. T.: Stratospheric ozone depletion and future levels of atmospheric chlorine and bromine, Nature, 344, 729-734, 1990.

Saiz-Lopez, A., and Fernandez, R. P.: On the formation of tropical rings of atomic halogens: Causes and implications, Geophysical Research Letters, 43, 2928-2935, 2016.

Salawitch, R. J., Weisenstein, D. K., Kovalenko, L. J., Sioris, C. E., Wennberg, P. O., Chance, K., Ko, M. K., and McLinden, C. A.: Sensitivity of ozone to bromine in the lower stratosphere, Geophysical research letters, 32, 2005.

Stutz, J., Werner, B., Spolaor, M., Scalone, L., Festa, J., Tsai, C., Cheung, R., Colosimo, S. F., Tricoli, U., Raecke, R., Hossaini, R., Chipperfield, M. P., Feng, W., Gao, R.-S., Hintsa, E. J., Elkins, J. W., Fahey, D., Moore, F. L., Daube, B., Pittman, J.,

Wofsy, S., and Pfeilsticker, K.: A New Differential Optical Absorption Spectroscopy Instrument to Study Atmospheric Chemistry from an High-Altitude Unmanned Aircraft, Atmospheric Measurement Techniques Discussions, Submitted, 2016.

Weidner, F., Bösch, H., Bovensmann, H., Burrows, J., Butz, A., Camy-Peyret, C., Dorf, M., Gerilowski, K., Gurlit, W., and Platt, U.: Balloon-borne limb profiling of UV/vis skylight radiances, O 3, NO 2, and BrO: technical set-up and validation of the method, Atmospheric Chemistry and Physics, 5, 1409-1422, 2005.

Werner, B., Stutz, J., Spolaor, M., Scalone, L., Raecke, R., Festa, J., Colosimo, S. F., Cheung, R., Tsai, C., Hossaini, R., Chipperfield, M. P., Taverna, G. S., Feng, W., Elkins, J. W., Fahey, D. W., Gao, R. S., Hintsa, E. J., Thornberry, T. D., Moore, F. L., Navarro, M. A., Atlas, E., Daube, B. C., Pittman, J., Wofsy, S., and Pfeilsticker, K.: Probing the subtropical lowermost stratosphere and the tropical upper troposphere and tropopause layer for inorganic bromine, Atmos. Chem. Phys., 17, 1161-1186, 10.5194/acp-17-1161-2017, 2017.

Wofsy, S. C., McElroy, M. B., and Yung, Y. L.: The chemistry of atmospheric bromine, Geophysical Research Letters, 2, 215-218, 1975.

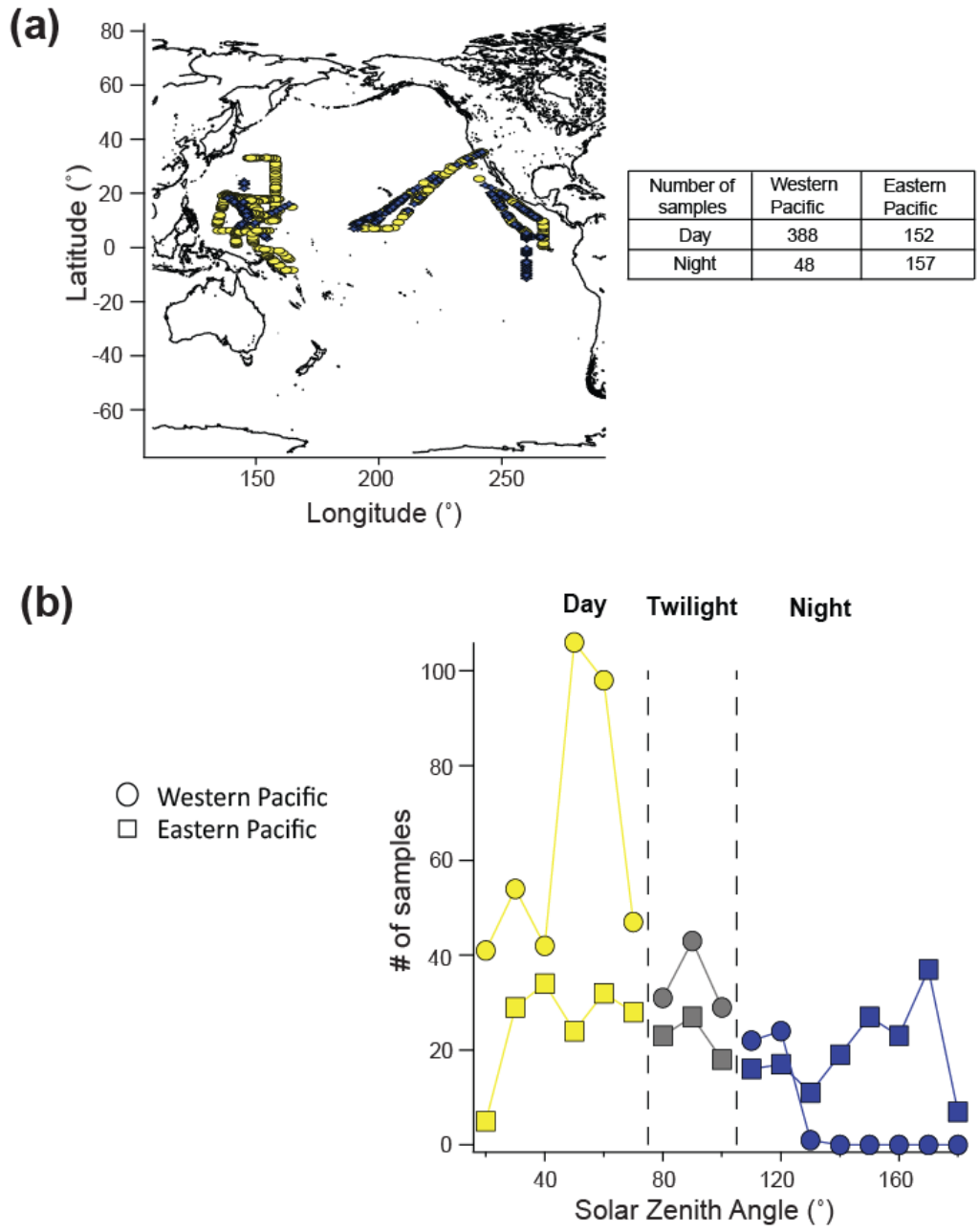

Number of samples	Western Pacific	Eastern Pacific
Day	388	152
Night	48	157

Figure 1: (a) Location of GWAS observations along ATTREX flight tracks taken at different altitudes over WP and EP. Yellow filled circles represent the samples taken during the day and blue filled circles the samples taken at night. (b) Sample density of GWAS observations arranged by solar zenith angle over the western and eastern Pacific. Yellow filled circles represent samples taken over WP during daylight, while blue filled circles are the samples taken over WP during night-time. Yellow filled squares represent the samples taken over EP during daylight, while blue filled squares are the samples taken over EP during night-time. Grey circles and squares are the samples taken during twilight over WP and EP, respectively.

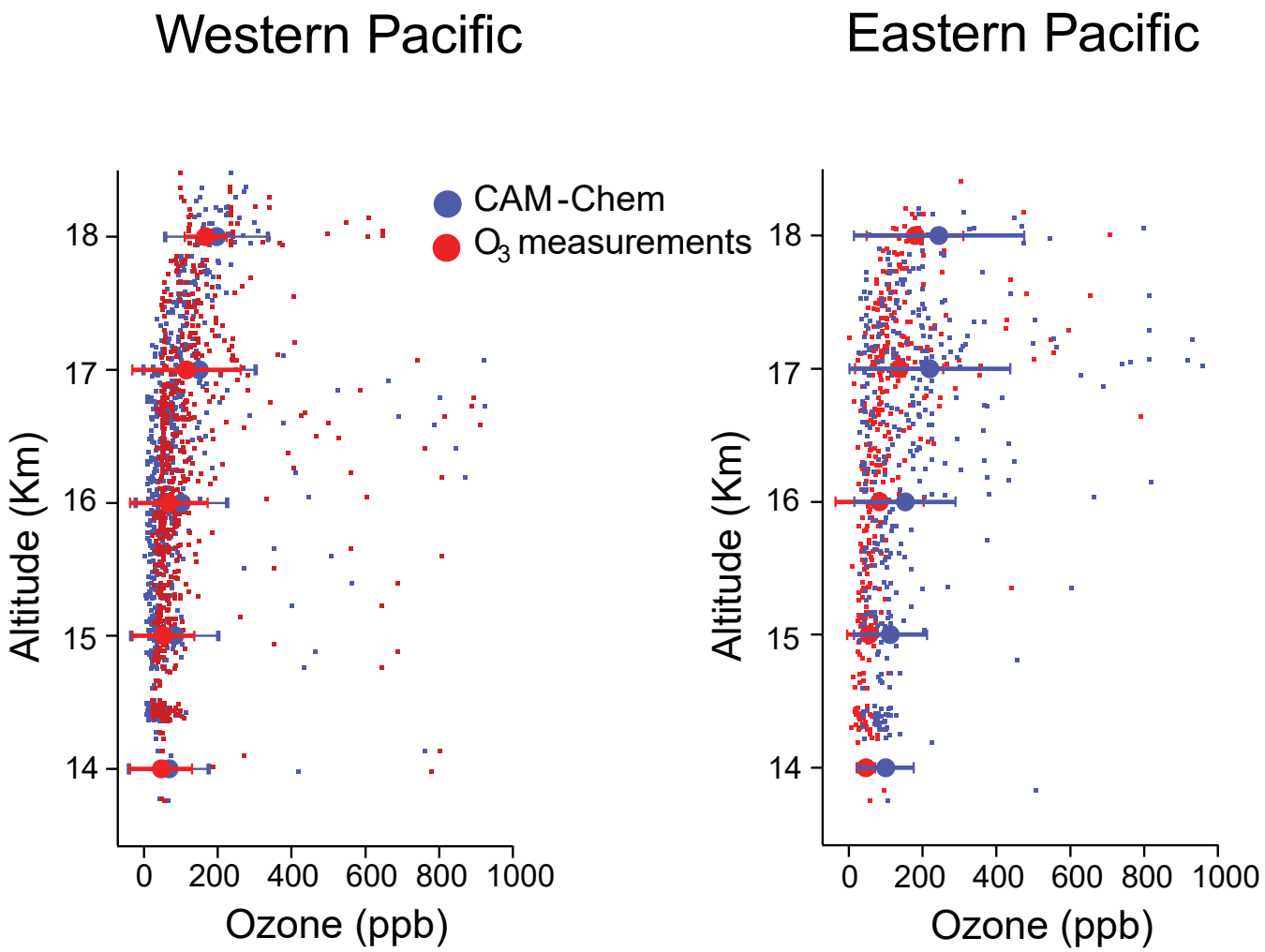

Figure 2: NOAA-UCATS O_3 observations for all flights (blue dots) and CAM-Chem simulations along ATTREX flight tracks (red dots). Filled circles represent the mixing ratios averaged into 1 km altitude bins ± 1 sd over WP and EP to observe the tendency of the mixing ratios as the altitude increases. Range of the bins are: 14 km= 13.5 to 14.5 km, 15 km= 14.5 to 15.5 km, 16 km= 15.5 to 16.5 km, 17 km= 16.5 to 17.5 km, 18 km= 17.5 to 18.5 km. Similar figures for CH_2Br_2 and $CHBr_3$ are in Navarro et al., (2015).

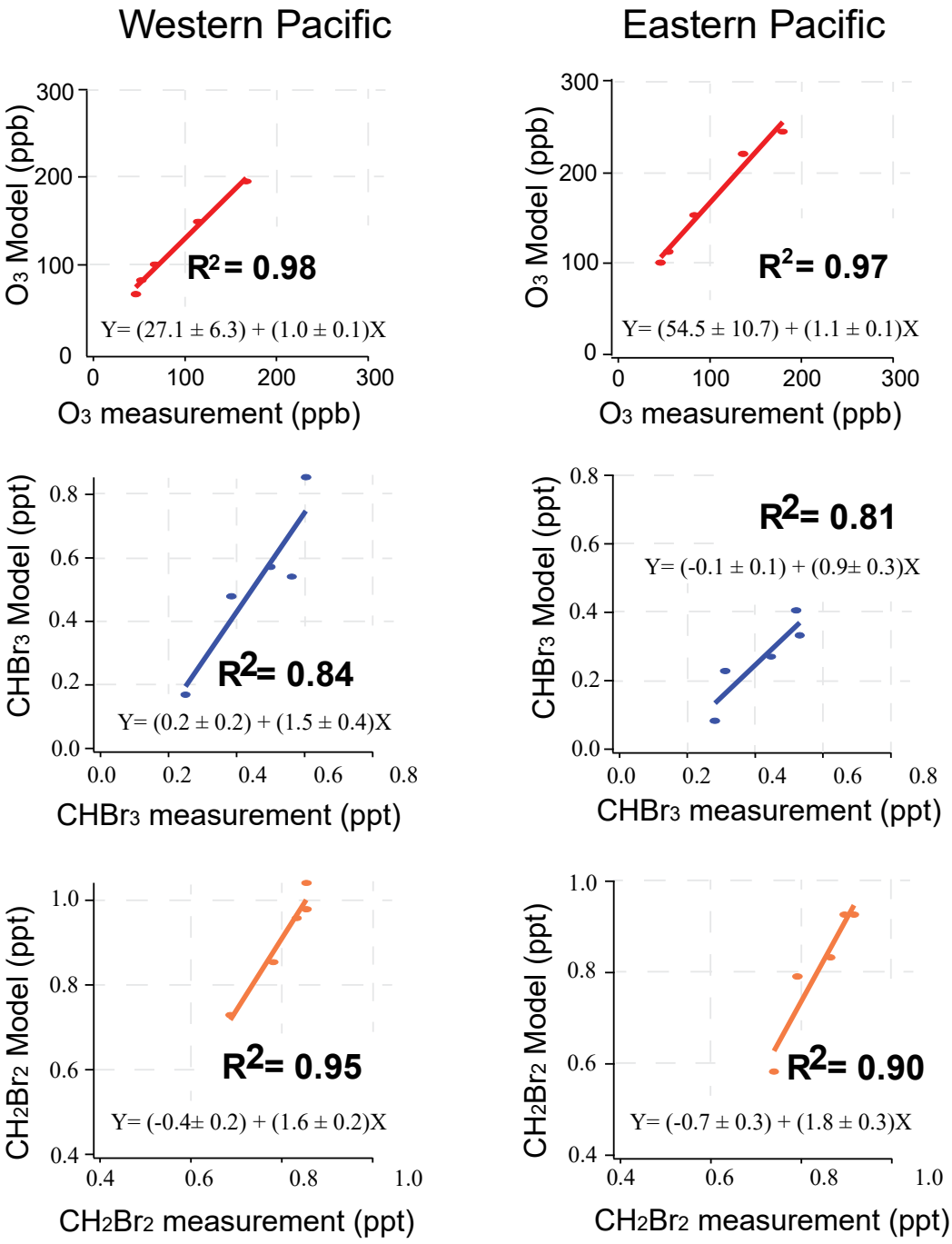

Figure 3: Correlations between measured and modelled mixing ratios of O_3, $CHBr_3$ and CH_2Br_2 over the WP and EP, respectively, using the 1 km average bins. Filled circles are the mixing ratios averaged into 1 km altitude bins (same as in figure 1 for O_3, and figure 1 in Navarro et al., (2015) for $CHBr_3$ and CH_2Br_2). Solid lines represent the linear regression analysis of the 1 km average bins including coefficient of determination (R^2) and regression equation (Y).

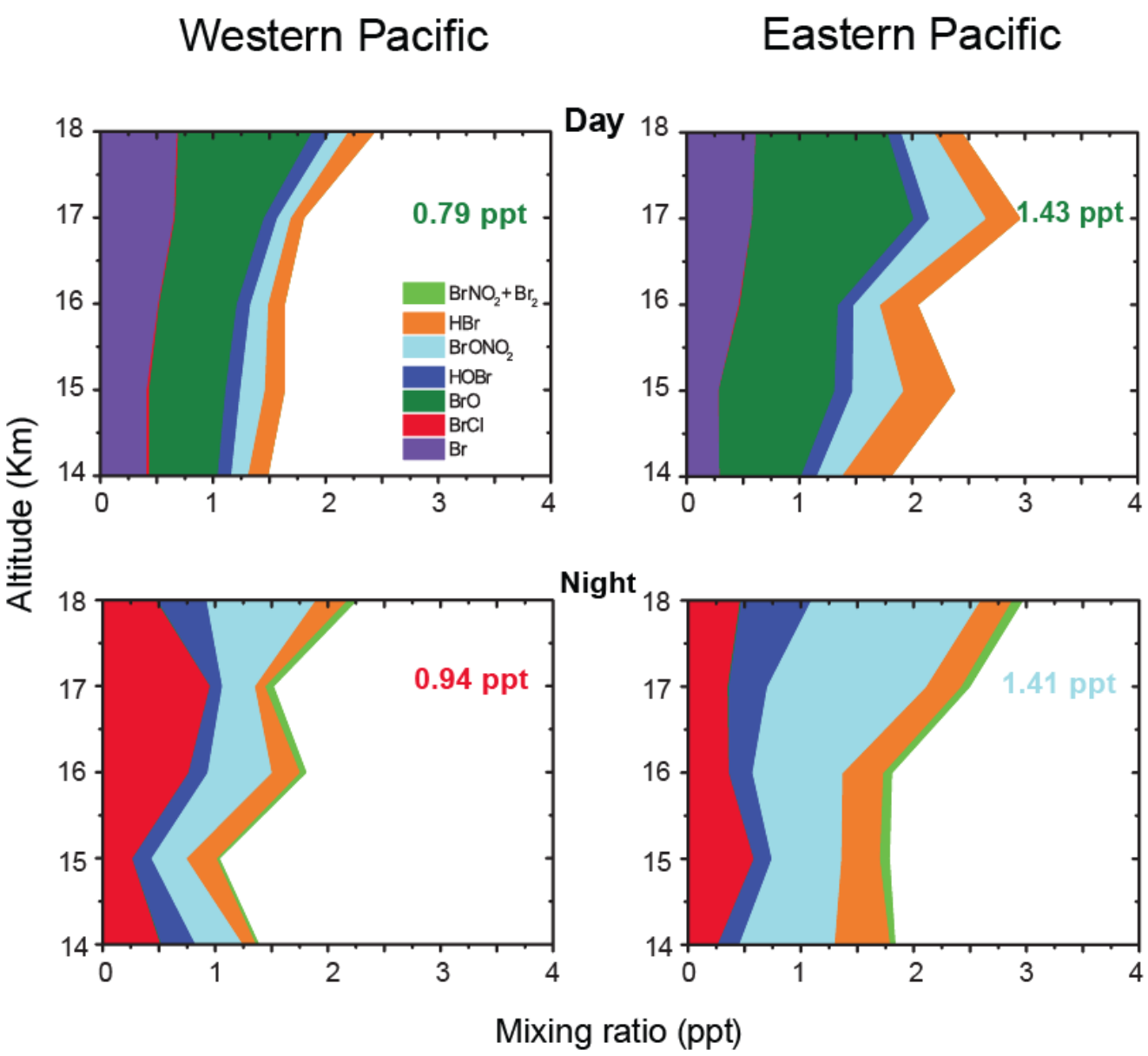

Figure 4: Model calculations of inorganic bromine partitioning along ATTREX flight tracks over the WP and EP using CAM-Chem with prevailing atmospheric conditions (specified meteorology) during the ATTREX campaign. Numbers inside the boxes represent the mixing ratios of BrO (green), BrCl (red) and $BrONO_2$ (light blue) at 17 km.

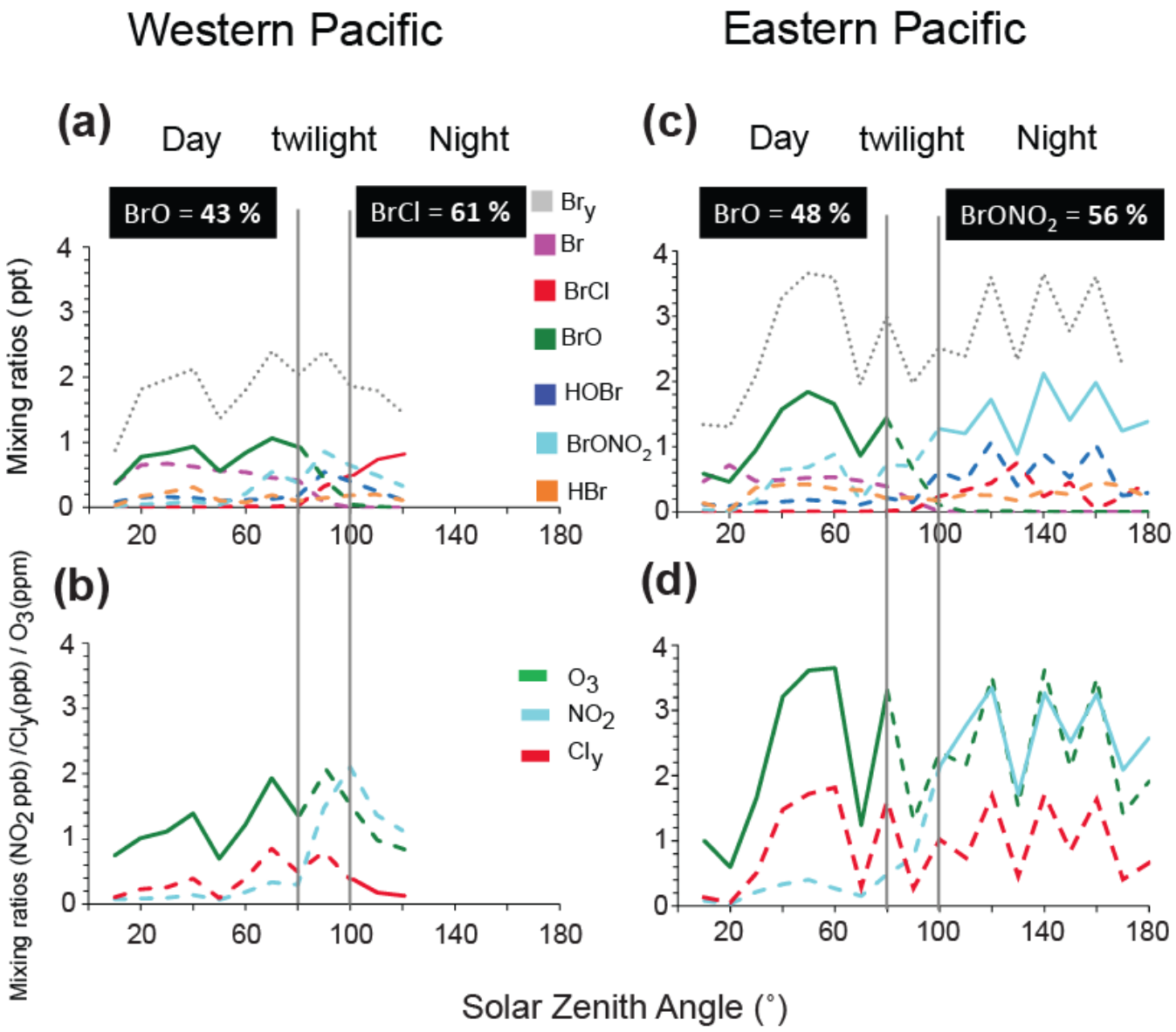

Figure 5: Average of inorganic bromine species (top panel) and main reactants of the inorganic chemistry (bottom panel) using the entire range of altitudes (14 to 18 km) over the western Pacific (a and b) and eastern Pacific (c and d). Black boxes indicate the percentage of the dominant Br_y species for day and night at 17 km.

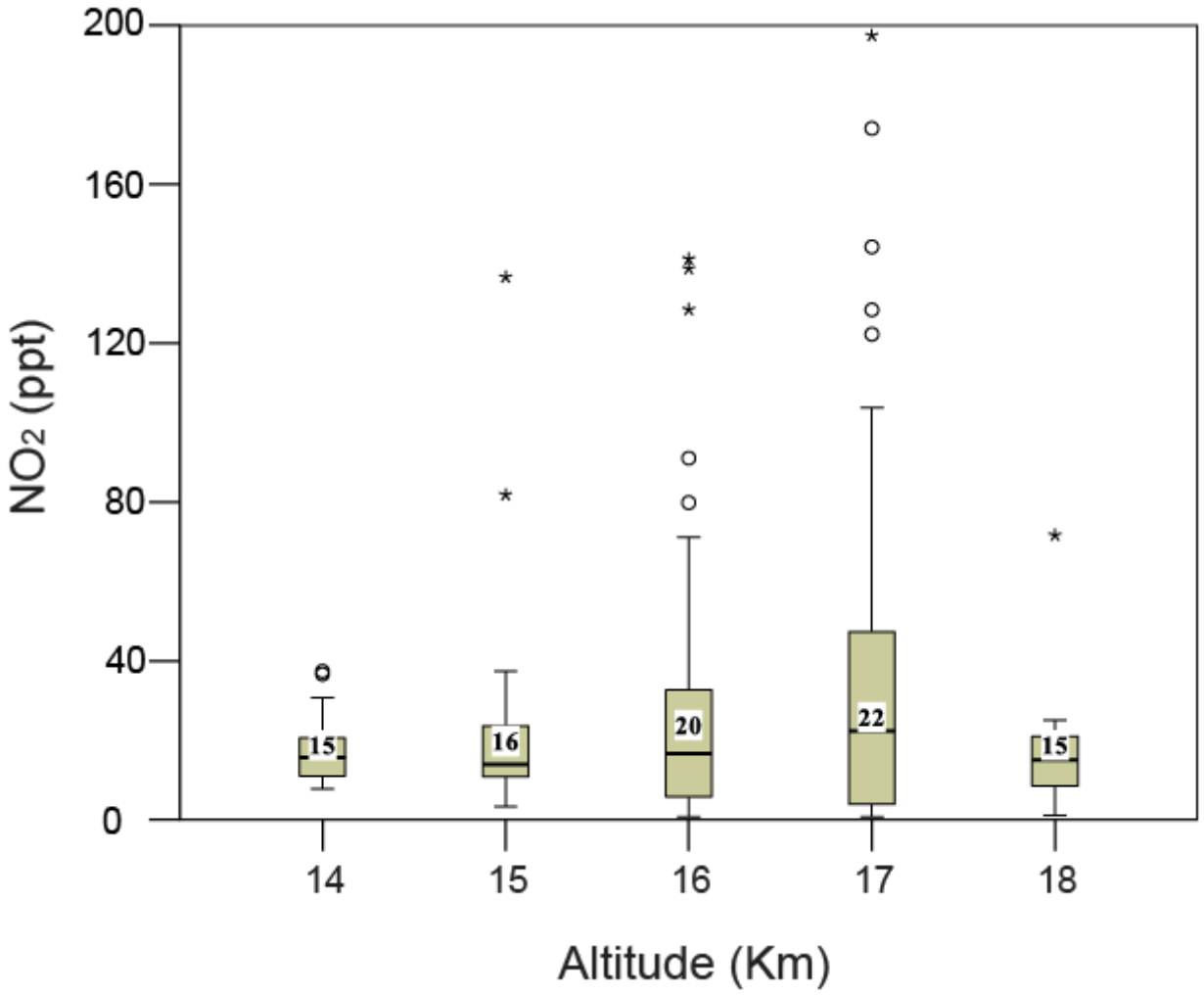

Figure 6: Boxplot of CAM-Chem NO_2 estimations as a function of altitude during daylight over eastern Pacific. The filled boxes display the minimum, first quartile (Q1), median (Q2), third quartile (Q3), and maximum values. Black line across the interior of the box represent the median (Q2) of NO_2 for the corresponding altitude. The bottom of the box is the first quartile (Q1) or the 25th percentile (the middle value between the smallest number and the median of the data set), while the top of the box is the third quartile (Q3) or the 75th percentile (the middle value between the median and the highest value of the data). T-bars extended from the boxes represent the whiskers (the largest and the smallest non-outlier value, respectively). Circles and stars are the outliers defined according to the interquartile range (IQR = Q3-Q1): Circles are the "out values" or the NO_2 mixing ratios greater than 1.5 times the interquartile range, and starts are "the extreme values" or the NO_2 mixing ratios greater than 3 times the interquartile range. The numbers inside the box represent the average NO_2.

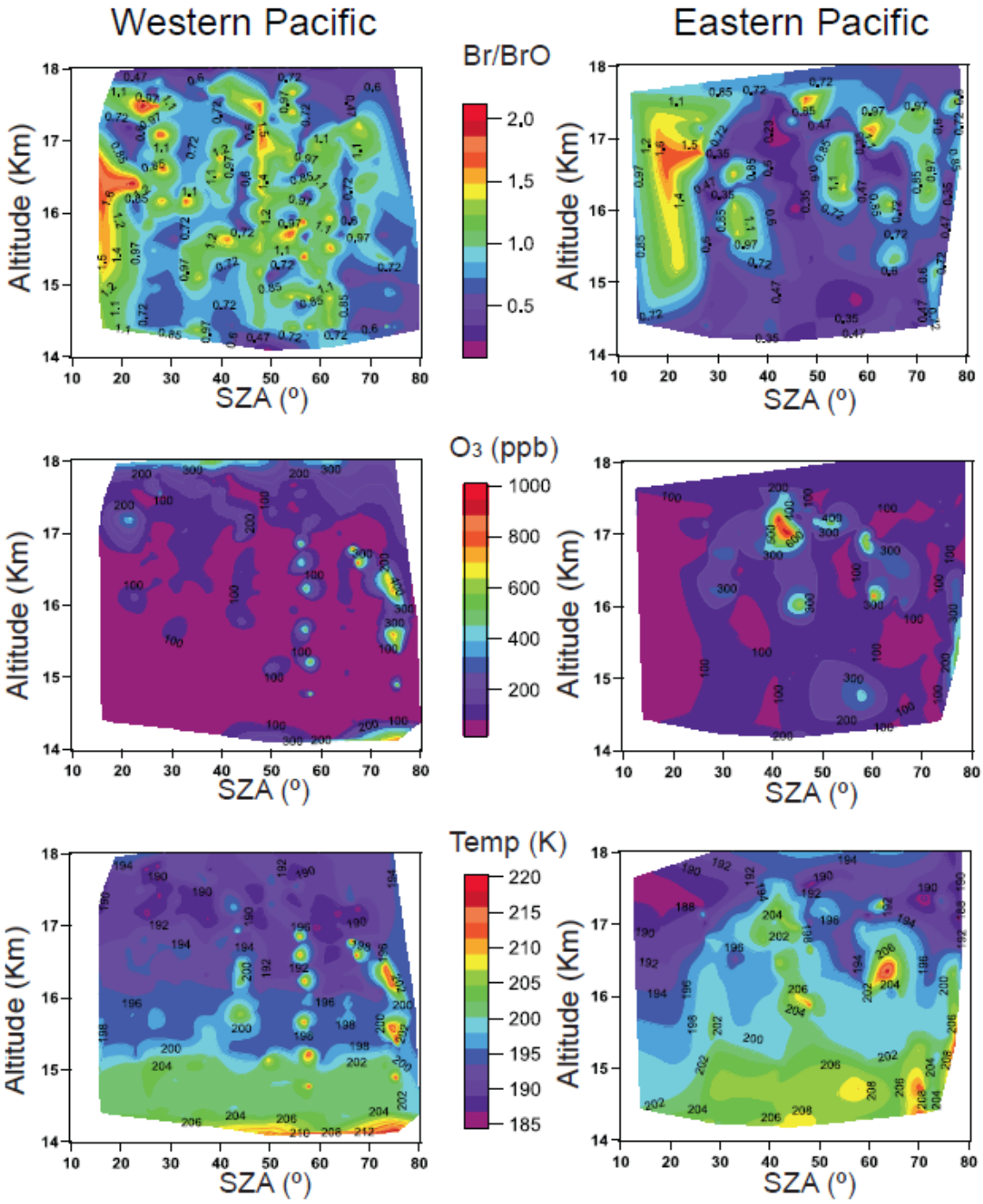

Figure 7: Modelled estimations of the daylight Br/BrO ratio (top panel), ozone (middle panel) and temperature (bottom panel) as function of SZA over the WP and EP using CAM-Chem.

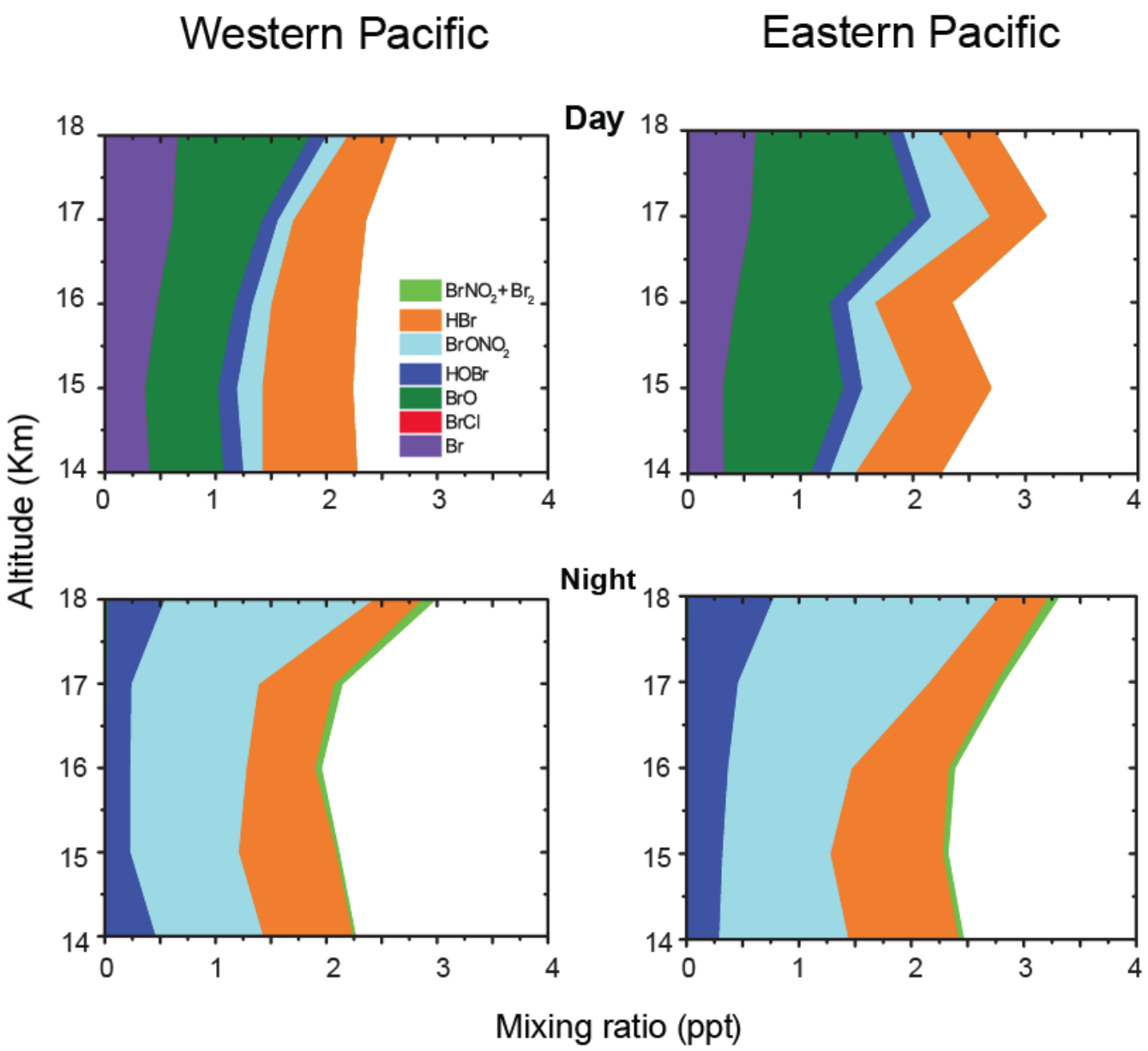

Figure 8: Inorganic bromine partitioning along ATTREX flight tracks over the western and eastern Pacific. Similar to Fig 4, but turning off the ice aerosol recycling reactions in the CAM-Chem chemical mechanism.

5

Table 1: Summary of the results found at the Tropical Tropopause level (~17km)

	Specie (time)	**WP (ppt)**	**EP (ppt)**
Mean	BrO (day)	0.79	1.43
	Br (day)	0.64	0.57
	BrCl (night)	0.94	0.34
	BrONO2 (night)	0.29	1.41
#Range	O_3 (day)*	35-500	35-900
	NO_2 (day)	1-227	0.7-343
	Cl_y (day)	1-515	1-969
	Temp (day)**	188-192	188-206

Range defined as min and max values, *units in ppb, **units in K.

Supplementary information for:

Modelling the Inorganic Bromine Partitioning in the Tropical Tropopause over the Eastern and Western Pacific Ocean.

Maria A. Navarro[1], Alfonso Saiz-Lopez[2], Carlos A. Cuevas[2], Rafael P. Fernandez[3], Elliot Atlas[1], Xavier Rodriguez-Lloveras[2], Douglas Kinnison[4], Jean-Francois Lamarque[4], Simone Tilmes[4],Troy Thornberry[5,6], Andrew Rollins[5,6], James W. Elkins[5], Eric J. Hintsa[5,6], and Fred L. Moore[5,6]

[1] Department of Atmospheric Sciences, RSMAS, University of Miami, Miami, Florida, USA
[2] Department of Atmospheric Chemistry and Climate, Institute of Physical Chemistry Rocasolano, CSIC, Madrid, Spain
[3] National Research Council (CONICET), FCEN-UNCuyo, UTN-FRM, Mendoza, Argentina
[4]Atmospheric Chemistry Observation & Modeling Laboratory, National Center for Atmospheric Research, Boulder, Colorado, USA
[5] National Oceanic & Atmospheric Administration, Earth System Research Laboratory, Boulder, Colorado, USA
[6] Cooperative Institute for Research in Environmental Science, University of Colorado, Boulder, Colorado, USA

Correspondence to: Maria A. Navarro (mnavarro@rsmas.miami.edu)

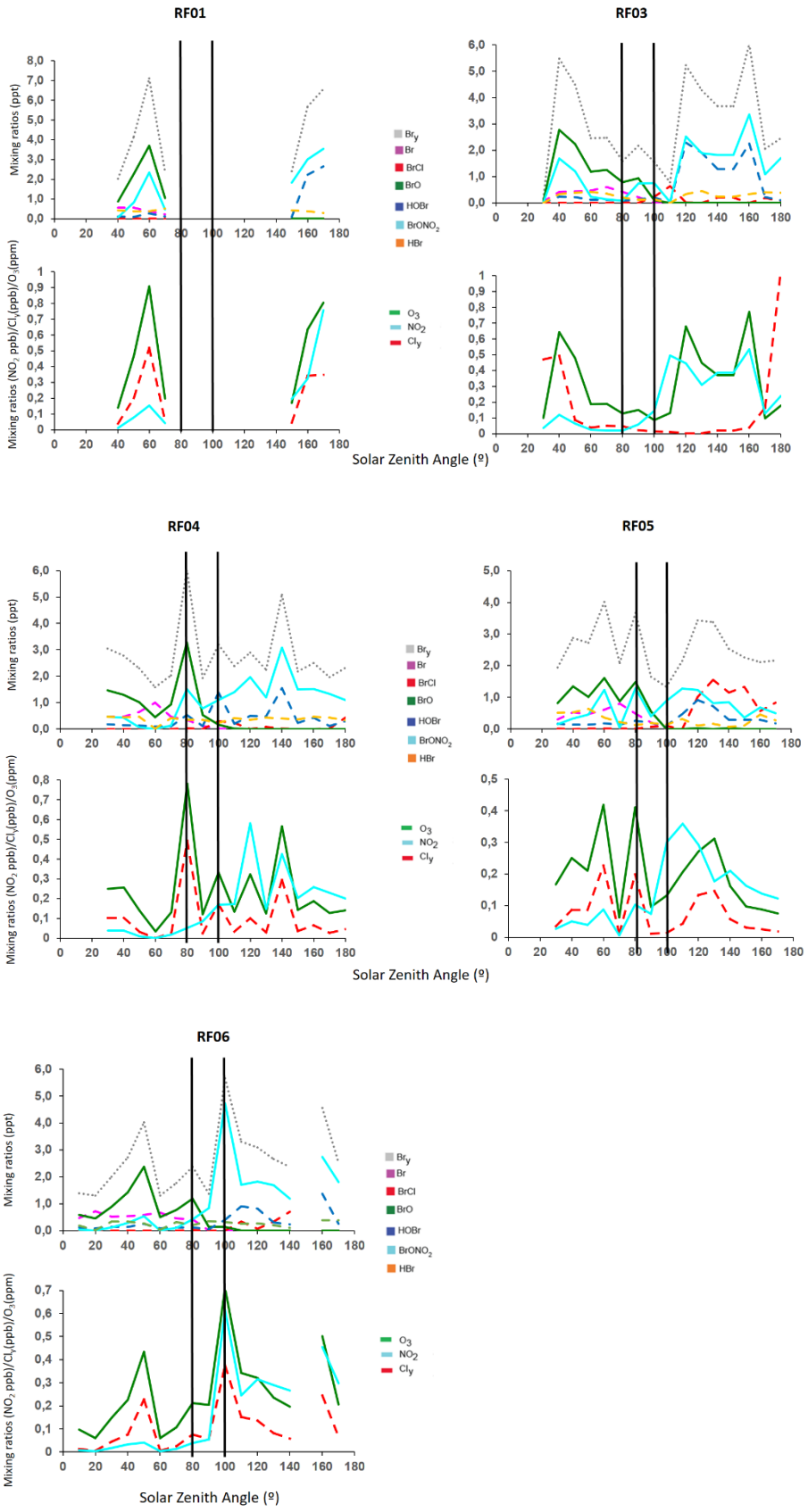

Figure S1: inorganic bromine species and main reactants of the inorganic chemistry using the range of altitudes (14 to 18 km) over the eastern Pacific for flights RF01, RF03, RF04, RF05 and RF06.

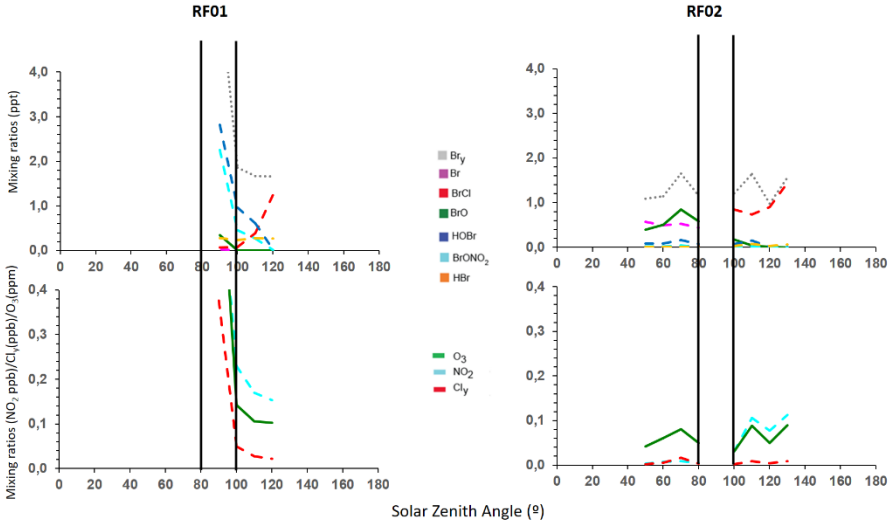
RF01
RF02
Mixing ratios (ppt)
Mixing ratios (NO2, ppb)/Cly(ppb)/O3(ppm)
Bry
Br
BrCl
BrO
HOBr
BrONO2
HBr
O3
NO2
Cly
Solar Zenith Angle (º)

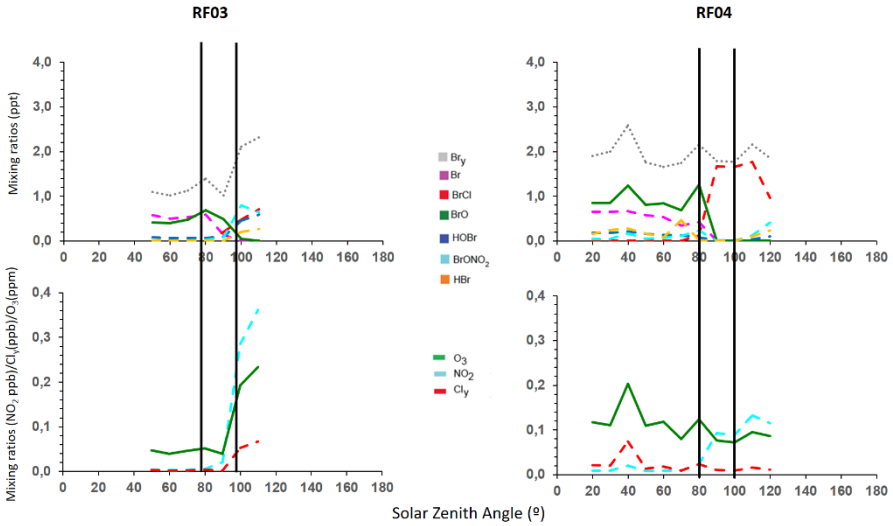
RF03
RF04
Mixing ratios (ppt)
Mixing ratios (NO2, ppb)/Cly(ppb)/O3(ppm)
Bry
Br
BrCl
BrO
HOBr
BrONO2
HBr
O3
NO2
Cly
Solar Zenith Angle (º)

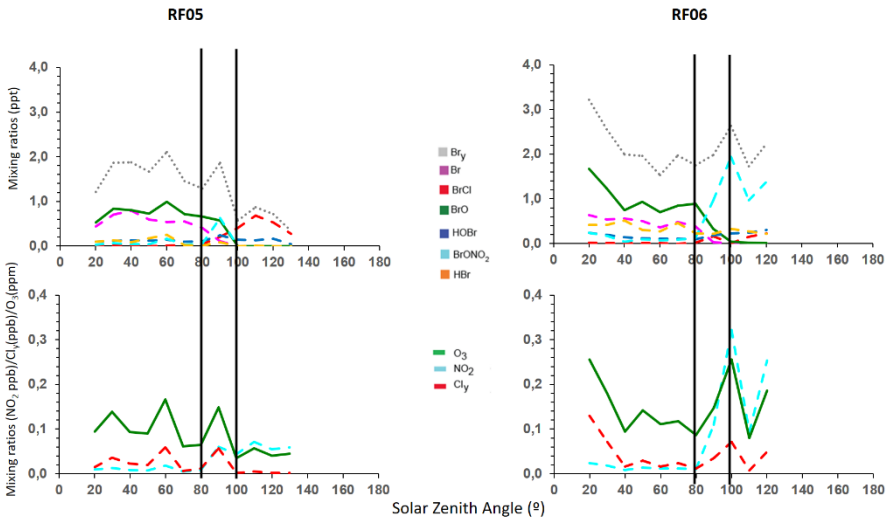
RF05
RF06
Mixing ratios (ppt)
Mixing ratios (NO2, ppb)/Cly(ppb)/O3(ppm)
Bry
Br
BrCl
BrO
HOBr
BrONO2
HBr
O3
NO2
Cly
Solar Zenith Angle (º)

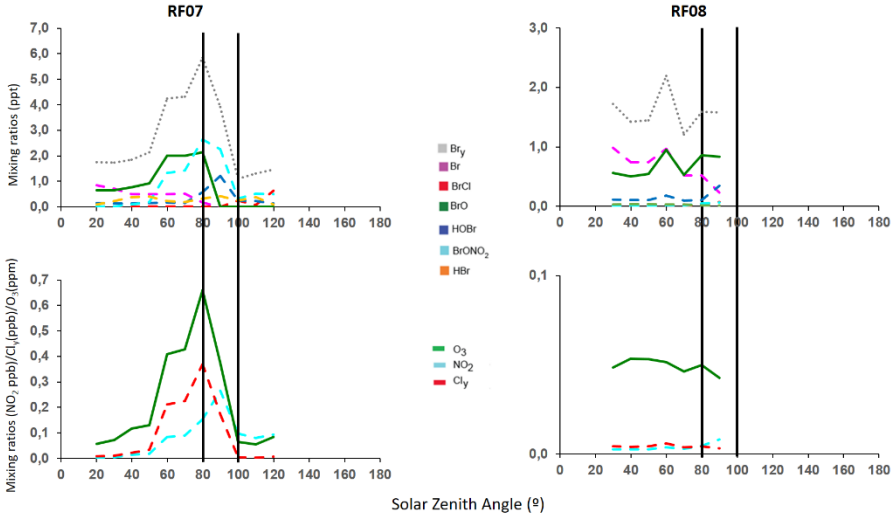

Figure S2: inorganic bromine species and main reactants of the inorganic chemistry using the range of altitudes (14 to 18 km) over the western Pacific for all flights.